Bulletin of the Geological Society of Malaysia, Volume 73, May 2022, pp. 139 - 149
DOI: https://doi.org/10.7186/bgsm73202211

Geophysics and geomorphic observation for near-surface structures mapping of Seulimeum Fault on Lamtamot area, Northern Sumatra

Muhammad Yanis[1], Gozian Islami[1], Nazli Ismail[1,2,*]

[1] Department of Geophysical Engineering, Faculty of Engineering, Universitas Syiah Kuala, Darussalam-Banda Aceh 23111, Indonesia
[2] Department of Physics, Faculty of Mathematics and Natural Sciences, Universitas Syiah Kuala, Darussalam-Banda Aceh 23111, Indonesia
* Corresponding author email address: nazli.ismail@unsyiah.ac.id

Abstract: In the northern part of Sumatra Island, Indonesia, the Great Sumatran Fault, which can cause an earthquake, was divided into two segments: the Aceh and Seulimeum. An effort to reduce the risk is mapping the fault area, especially in the region that does not clearly show the sign on the surface, e.g., in the Lamtamot area, Indonesia. Electrical resistivity is widely used to study shallow structures, but the method requires more time when applied in a large area. This research explores the potential of an extremely low frequency (very low frequency-electromagnetic; VLF-EM) method to investigate the shallow fault of the Seulimeum segment. Here, the VLF-EM is compared with other geophysical methods such as resistivity and magnetic methods. For comprehensive results, the geomorphic observation that was conducted covered outcrops of the fault and trenching sites in the geophysical study for validating the model. A similar pattern of the VLF-EM and electrical resistivity data has been shown in a two-dimensional profile using data processing. The fault structure can be mapped at a distance of 20–24 m from the profile measurement, which is demonstrated by the low current density associated with the conductive zone from the VLF-EM, and low resistive anomaly in electrical resistivity. The fault can also be confirmed via magnetic intensity, which significantly increases at the same distance (20–25 m) of the VLF-EM and electrical resistivity. The geomorphic observation shows outcrops of fault activity, such as fault scarp, fractures, and faults, in the same direction as the Seulimeum segment, while scrap extends in the northwest direction up to ~20 m around the geophysical surveys. As revealed by the results, the VLF-EM method combined with other geophysical surveys and geomorphic observation can be used as a technique to image the fault that shows the shallow structure of the Seulimeum fault at 20–32 m along the profile.

Keywords: Near-surface geophysics, Seulimeum segment, VLF-EM, resistivity, fault structure

INTRODUCTION

The Great Sumatran Fault (GSF) is a right-lateral strike-slip fault that extends ~1900 km from the southern tip of Sumatra to the Andaman Sea. Such a long fault system splits into 20 segments (Sieh & Natawidjaja, 2000; Ito *et al.*, 2012; Yanis *et al.*, 2020). Several earthquake events have been recorded in the southern part of Sumatra due to the GSF activity. In contrast, the northern part has never shown significant seismic activities for more than 170 years. The fault and its activity can cause a ≥ 7 M_w earthquake if the energy stored within the Earth is not released (Ito *et al.*, 2012). This is a significant threat for the Aceh Province's future because the potential earthquake affects infrastructures and human life, even when the magnitudes are considerably small.

Regarding the process, the earthquake will not spontaneously dissipate the energy, neither will it have one major earthquake only, but their aftershocks will emerge on smaller and larger scales. Two significant earthquakes in Aceh Province occurred in Tangse, October 22, 2013, by 5.6 M_w, and Pidie Jaya, December 7, 2016, by 6.5 M_w, which should give a valuable lesson for disaster mitigation. The earthquake activity has repeatedly occurred with disastrous damage to infrastructure and many fatalities (Muzli *et al.*, 2018; Marwan *et al.*, 2019a). To reduce earthquake hazards, we need to map the active fault, especially in the location that does not show the fault trace on the surface, i.e., those earthquakes caused by sedimentation and erosional processes such as those found in the Lamtamot village, which is 60 km away from the east of Banda Aceh, the capital city of Aceh Province, Indonesia. According to (Marwan *et al.*, 2019b; Rizal *et al.*, 2019), the geology of the research area is dominated by volcanic rocks, comprising basaltic and andesite rock formations, volcanic breccia, tuffs, and agglomerates. The uppermost layer is covered by fluvial deposits, which are mainly used as a rice paddy field. The northern part of the GSF splits into two segments: Aceh and Seulimeum faults. The fault passes along the east side

0126-6187; 2637-109X / Published by the Geological Society of Malaysia.

of Banda Aceh through the Seulawah Agam volcano to the Weh Island and the Andaman Sea. Figure 1 shows a simple sketch of the research area in Aceh Province.

Generally, the electrical resistivity (ERT) method is a geophysical technique widely used to study shallow structures in the subsurface, such as shallow fault studies (Ismail *et al.*, 2017), soil characteristics in the depth of less than 100 m (Chabaane *et al.*, 2017; M. Yanis *et al.*, 2019), and natural disasters such as landslide (Bichler *et al.*, 2004). The ERT works by injecting an electric current from the surface into the ground with various electrode configurations. It also provides precise results, and it is very easy to process the data. However, it requires a relatively long time when applied in a large area and requires high mobility in the data acquisition process (Khalil *et al.*, 2009; Yanis *et al.*, 2017). Additionally, in some areas where the mobility to collect data is difficult, the resistivity method is relatively complicated to operate. Furthermore, another technique in near-surface geophysics, such as magnetic and gravity, has been applied in several fault studies (Nasuti *et al.*, 2012). However, this method has the problem of data ambiguity for 2D inversion to estimate the depth information. Therefore, it is necessary to develop a more robust method that has a very low frequency such as an electromagnetic (VLF-EM) method, which can be used in complex fields. Compared with the conventional ERT method, the VLF-EM can be used only by one person, thereby reducing time consumption.

The VLF transmitters operate in the frequency bandwidth of 15–30 kHz and transmit military communications for 24 h to become an electromagnetic source for geophysical investigations (Gürer *et al.*, 2009). Subsurface conductors may be removed using a VLF receiver. The VLF method has been successfully used to investigate faults in another place, e.g., the buried faults of Fethiye–Burdur Fault Zone, Turkey (Gürer *et al.*, 2009) and in Northern Norway for identifying the Stuoragurra Fault (Olesen *et al.*, 1992). The VLF-EM can also be applied in other instances, such as in the LUSI embankment for landslides study (Sungkono *et al.*, 2014), in estimating the structure of the archaeological site (Abbas *et al.*, 2012; Yanis *et al.*, 2017), and for geothermal prospecting (Baranwal & Sharma, 2006). In this research, the VLF-EM is used as an alternative method to investigate the shallow structures of the fault in the Seulimeum segment. The method also compares electrical resistivity and magnetic methods measured along the same profile. The geomorphic observation is conducted around the research area to search the Seulimeum fault trend; this aims to validate the geophysical model in the subsurface. The observation covers outcrops of the fault activity in the Lamtamot area and trenching site in the same location as the geophysical study.

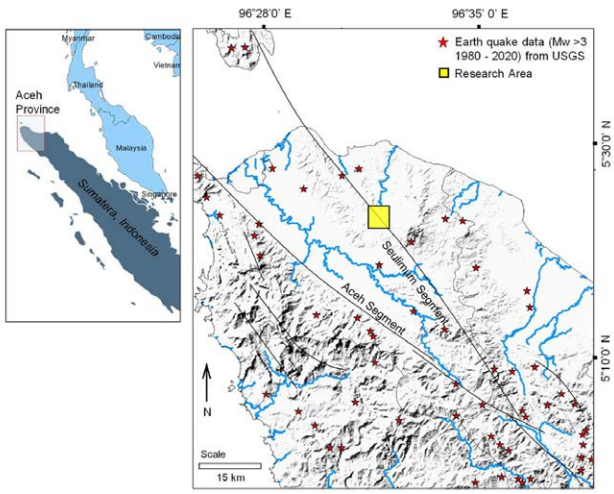

Figure 1: Aceh is one of the Indonesian provinces located at the northern tip of Sumatra. The seismicity data from the US Geological Survey (1980–2020) shows the distribution of ≥5 M_w earthquakes in several places relatively close to the Great Sumatran Fault fault, especially in the Aceh and Seulimeum segments (USGS, 2020). The yellow box is represented as near-surface geophysical research in Lamtamot village, Aceh Besar.

BACKGROUND AND GEOLOGICAL SETTINGS

The GSF is one of the most extensive strike-slip fault types located on the island of Sumatra, and the fault is ~400 km from the northeast of the Sunda Trench (Sieh & Natawidjaja, 2000; Yanis *et al.*, 2020). Generally, this fault is divided into 19 segments, starting from the southern part with a small strike-slip and increases to the northern part of Sumatra Island. Most of the 19 segments have had earthquake seismicity for the last century, with a magnitude between 6.0 and 7.7. However, two segments in the northern part of Sumatra: the Aceh and Seulimeum segments, have no earthquake seismicity (Natawidjaja & Triyoso, 2007; Ito *et al.*, 2012). In fact, one of these segments passes through crucial places, such as public infrastructures, mosques, archaeological objects, and settlements as well as cities of Banda Aceh and Aceh Besar. The seismicity gap for 170 years along 200 km can cause a considerable earthquake hazard in these segments (Sieh & Natawidjaja, 2000; Natawidjaja & Triyoso, 2007; Ito *et al.*, 2012). Thus, near-surface geophysical research is essential to study the detailed fault characteristics in these segments. Based on the geological map shown in Figure 2(a), the rock deformations in the Seulimeum segment are dominated by sedimentary and volcanic rock, consisting of Lamteuba volcanic rock andesite to dacite, breccia, tuff, agglomerates, and dust flow. In contrast, the Aceh segment contains igneous rock and continental sediment bedrock.

The global gravity data from satellite Topex is presented to show the density contrast that corresponds to Seulimeum and Aceh segments, as shown in Figure 2(b) The data resolution of Topex gravity is 1.8 km for one pixel (Chatterjee *et al.*, 2007; Yanis *et al.*, 2019). Gravity is a geophysical exploration method to measure variations in the Earth's gravitational field, which occurs due to differences in mass density between rocks below the surface, and it is

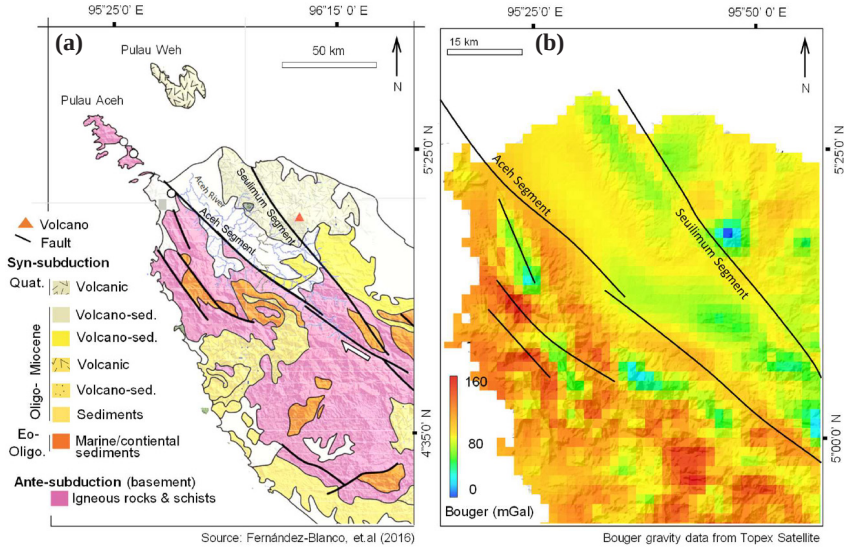

Figure 2: (a) Geological map of the research area that shows the main control units of the fault structure (syn-subduction) on top of the basement ante-subduction (Fernández-Blanco *et al.*, 2016), whereas (b) is a Bouger anomaly map obtained from the analysis of the global gravity Topex with a resolution of 1.8 km for 1 px. These data have been analyzed by (Yanis *et al.*, 2019) to map the regional fault of Sumatra Island.

also influenced by topographic differences above the Earth's surface (Kamesh Raju *et al.*, 2007; Ma & Li, 2012; Yanis & Marwan, 2019). Based on the analysis, the Bouguer gravity shows the rock contrast, which correlates with the GSF segments ranging from 0 to 160 mGal. Generally, the Bouguer data are relatively high in the Aceh and Seulimeum segments. Furthermore, the low anomalies are only obtained simultaneously in several places with high topography, such as the Seulawah Agam volcano. Specifically, the Bouguer data are dominated by a lower value in the north side from 40 to 90 mGal, in response to the contrast of volcanic rock and the fault structure of the Seulimeum segment.

Further, the high Bouguer anomaly is dominated in the Aceh segment area ranging from 40 to 160 mGal in response to igneous rock. However, the global gravity data can show the contrast anomaly between the Aceh segment that extends to the Andaman Islands and the Seulimeum segment that leads to the Weh Island. The anomaly contrast is obtained with a significant difference in topography between both segments, and the Bouguer anomaly is confirmed (Yanis *et al.*, 2021) by an advanced analysis of gravity satellite to map the Aceh and Seulimeum segment. Moreover, the data only show the fault in a regional area but do not efficiently analyze a local anomaly. Several near-surface geophysical methods should be applied to study more specific local faults.

BASIC THEORY OF GEOPHYSICAL METHODS

Geophysics has been widely applied to study shallow and deep faults around the world (Saibi *et al.*, 2012; Zhang *et al.*, 2015). Meanwhile, several methods can be used for shallow structures. In this study, we discuss how the combination of VLF-EM, resistivity, and magnetic data can provide information on shallow faults. The results can identify fault patterns that indicate a significant disturbance due to subsurface tectonic activity.

Very low frequency-electromagnetic

The VLF-EM method is a low-frequency technique with a range of 15–30 kHz using military communication signals. As an electromagnetic method (EM), the VLF-EM requires two coils: one as a transmitter, and the other as a receiver. The transmitter coil in EM induction works with a power supply that delivers an alternating current. It produces a magnetic field around it and will induce the subsurface's conductive medium. The magnetic field oscillated to influence the conductive body in- and out-phase parameters as data in the VLF Instrument. The secondary magnetic field depends on the condition of the subsurface material. The VLF-EM is an EM that uses a military radio transmitter as a primary electromagnetic field. The transmitter is utilized for communicating and navigating underwater submarines, and it operates at 15–30 kHz (Sundararajan *et al.*, 2006; Ebrahimi *et al.*, 2019).

The wave oscillation from the transmitter has a deep penetration in the subsurface, which spreads in other places and can be used as a transmitter in the VLF method (Ramesh Babu *et al.*, 2007). The signal detected by the receiver is the total magnetic field H_R from the primary field H_P which propagates through the air and the secondary field H_S as an induced magnetic field in the conductor. The magnitudes of H_S and H_R depend on space, time, and frequency (Bosch & Müller, 2001), as shown in Eq. 1.

$$H_R = |H_P| e^{iwt} + |H_S| e^{i(wt-\varphi)} \quad (1)$$

The transmitter frequency is f = (ω / 2π), and φ is the phase shift between primary and secondary components from the magnetic fields. This information can be processed to determine the conductor's size and conductivity below the Earth's surface. However, in vector, the components of the magnetic field can be expressed as in Eq. 2.

$$\begin{pmatrix} 0 \\ H_{RY} \\ H_{RZ} \end{pmatrix} = \begin{pmatrix} 0 \\ H_{PY} \\ 0 \end{pmatrix} + \begin{pmatrix} 0 \\ H_{SY} \\ H_{SZ} \end{pmatrix} \quad (2)$$

The data obtained from the VLF-EM method are in-phase and quadrature, which represents the ratio of H_{RZ}/H_{RY} and characterizes the resistivity distribution below the surface. The VLF method operates by assuming a two-dimensional (2-D) conductivity structure in the subsurface, where the x-direction functions are the geological strike and the direction of the VLF transmitter, to get a strong induction anomaly, and the y-axis is the measurement profile with the VLF-EM instrument measuring the vertical (Hz) and horizontal (Hy) components of the magnetic field. Each station can determine the scalar tipper B given by Hz = B Hy; the real and imaginary components are usually expressed as percentages (Khalil *et al.*, 2009; Abbas *et al.*, 2012). The polarization difference in the two magnetic parts can also distinguish resistive and conductive areas below the surface, which are characterized by the same polarity in the resistive anomaly with different phases in the conductive zone (Karcıoğlu, 2019).

Electrical resistivity

Electrical resistivity plays a crucial role in delineating fault structures around the world. The conventional DC survey measures the potential difference from four electrodes that were injected into the ground; A and B are the current electrodes connected by cable to the DC battery, while M and N are the potential electrodes connected to the voltage measuring device. At each data point, the current intensity (I) in the circuit and potential difference (ΔV) between the M and N electrodes are measured, then the current electrode is moved symmetrically with varying distances, resulting in resistivity at different depths (Pozdnyakova *et al.*, 2001; Niculescu & Andrei, 2019); the simple concept of electrical resistivity is shown Figure 3 as illustrated in (Niculescu & Andrei, 2019). Based on parameters I, ΔV, and K (as a geometric factor, which is influenced by the type of electrode), the apparent resistivity (ρa) of the subsurface can be calculated using Eq. 3.

$$\rho a = \mathrm{K}\ \Delta \mathrm{V/I} \quad (3)$$

Although the apparent resistivity data differ from the electrical resistivity data of the subsurface soil, there is a complex relationship between both data, which is an inversion problem. Therefore, the inversion process of electrical resistivity is conducted using RES2DIV software, and it works based on smoothness-constrained of the least-squares method (Loke & Lane, 2004). A suitable model can be built through the difference between the calculated and measured data using the Root Mean Square (RMS), as shown in Eq. 4.

$$RMS = \sqrt{\frac{1}{N}\sum \left(\frac{d_i - f_i(m)}{\varepsilon_i} \right)^2} \quad (4)$$

where N is the number of measurement points, d is the measurement data, *f*(m) is the forward model, and ε_i is the tolerance that is given in the RES2DINV software.

Magnetic method

Magnetic surveys are used to investigate subsurface structures using variations in the Earth's magnetic field caused by the magnetic properties of rocks (Telford *et al.*, 1990; Surya *et al.*, 2019). A situation where the magnetization of objects is highly dependent on the Earth's magnetic field is formed in the rock anomaly (Zainal *et al.*, 2019; Martí *et al.*, 2020). The magnetic material in the rock will get a magnetic force and create a magnetic induction, which is stated in Eq. 5 as

$$J_i = kT, \quad (5)$$

where J is the magnetization, k is the susceptibility of a magnetic material, and T is the induction field. Meanwhile, the total magnetic field measurement, including external and magnetization is called magnetic induction (B), expressed in Eq. 6 as

$$B = \mu_0 (1+k)H, \quad (6)$$

where μ_0 is the magnetic permeability in a vacuum, and H is the intensity of the magnetic field. Further, B is

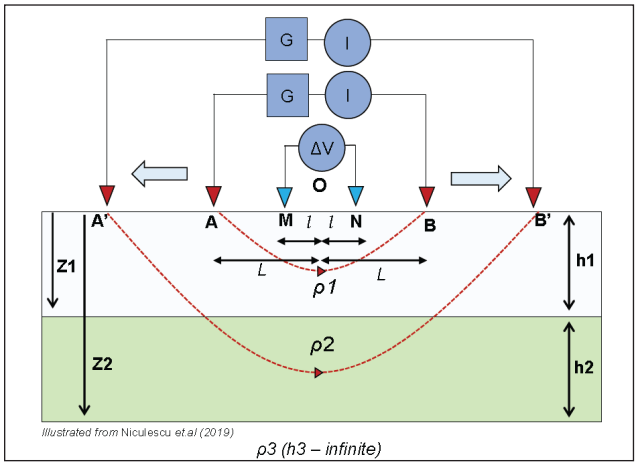

Figure 3: The concept of measuring the vertical electrical sounding method below the surface (Niculescu & Andrei, 2019). Wenner–Schlumberger electrode configuration; the dotted curve represents the current flow path, l = MN/2 is the half distance from the measuring electrode, L = AO = BO = AB/2 is the half distance from the current electrode.

a vector quantity whose amplitude can be measured. It is also called a total magnetic field.

FIELD MEASUREMENT

The research was conducted in the Lamtamot rice field (Figure 4) on the southern side of the Seulawah Agam volcano. The Lamtamot area contains a fluvial deposit where the shallow sediment has experienced disturbance due to farming. The VLF-EM data were measured along a profile in the east–west direction, i.e., almost perpendicular to the estimated Seulimeum fault in the NW–SE direction.

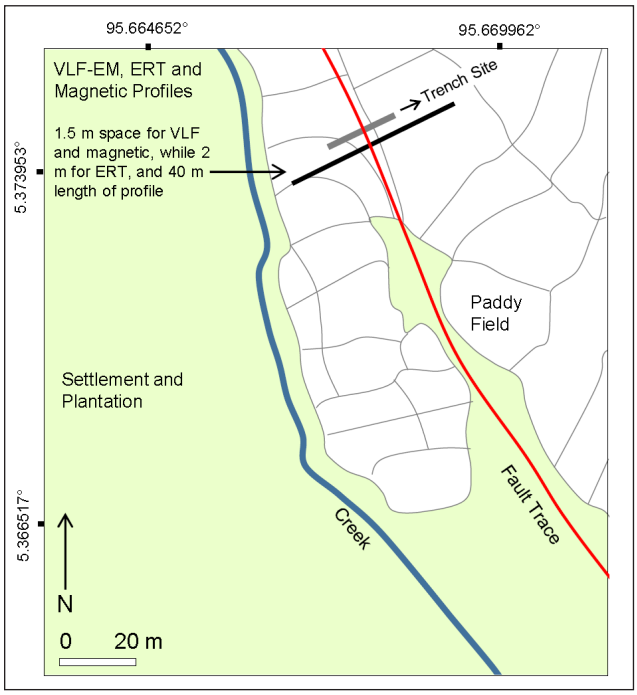

Figure 4: Description of field measurements showing very low frequency-electromagnetic, magnetic, and resistivity profile as a black line. The profile is made to cross the fault trace area of the Seulimeum segment obtained in the rice field's area.

Table 1: Data acquisition of geophysical methods.

No	Geophysical Methods	Parameter	Data
1.	Very Low Frequency-Electromagnetic	Number of Profile	1
		Sampling Station	2 m
		Length of Profile	42 m
		Frequency used	19.8 kHz
2.	Electrical Resistivity	Number of Profile	1
		Electrode Spacing	1.5 m
		Length of Profile	40 m
3.	Magnetic	Number of Profile	1
		Sampling Station	2 m
		Length of Profile	42 m

We acquired the ERT data along the same profile for the model comparison. The length of the profile was 42 m with a space of 2 m between stations for VLF-EM and magnetic measurement, whereas 1.5 m for ERT measurements; the specific description of geophysical measurements are shown in Table 1.

The VLF-EM and magnetic data were measured using the GEM GSM 19 instrument. The magnetic data and VLF-EM were measured simultaneously because they use the same equipment with different sensors. Instrumentally, the GSM 19 can simultaneously work with three frequencies in VLF mode, but we only use one, 19.8 kHz (NWC) from Exmouth, Western Australia. The reason is that only the NWC transmitter received good signal quality in the research area. Although they are 24 h available, in some remote areas the VLF signal is difficult to obtain. However, the tolerance limit for the VLF-EM method is 12%. The geological map also shows that the Seulimeum segment is perpendicular to the NW–SE direction. The transmitter position in relation to the fault direction is NWC Australia and JJI Japan. The VLF transmitter operates for 24 h, but some transmitters are turned off for maintenance with a predetermined schedule. Therefore, the data retrieval time must be adjusted to the maintenance schedule of each VLF transmitter station (GEM Systems, 2015). The resistivity data were obtained using the SuperSting R8 instrument with the configuration of Wenner–Schlumberger, the configuration is sensitive to the lateral and horizontal anomaly in the subsurface. The specific result of the ERT in this research was discussed by Ismail (Ismail *et al.*, 2017).

At the same location as both methods, the magnetic field is also acquired for delineating the near-fault using the GEM instrument by adding a proton precession magnetometer sensor; the standard correction of magnetic field data such as diurnal correction, and regional correction using International Geomagnetic Reference Field is applied to obtain a total magnetic field anomaly. However, since the magnetic field anomaly is a dipole, the field data must be reduced to become a monopole. Hence, the Seulimeum segment fault can be directly interpreted. To provide comprehensive results, the geomorphic observation covered the finding of fault outcrops in the Lamtamot area and conducted the trenching site in the same site as the geophysical location. This is shown in Figure 4 with the gray line, which extends for 4 m, and a depth of 1 m excavation in the subsurface.

RESULTS AND DISCUSSION

Geomorphic field observation

Based on the observation along the Seulimeum segment, several geological objects have been found in the research area, which supported the tectonic activity. We have identified the geomorphic features and fault outcrops in Lamtamot village and around the Seulimeum segment, as shown in Figure 5. In the southern part, there is an outcrop in the form of a fracture zone, which is perpendicular to the

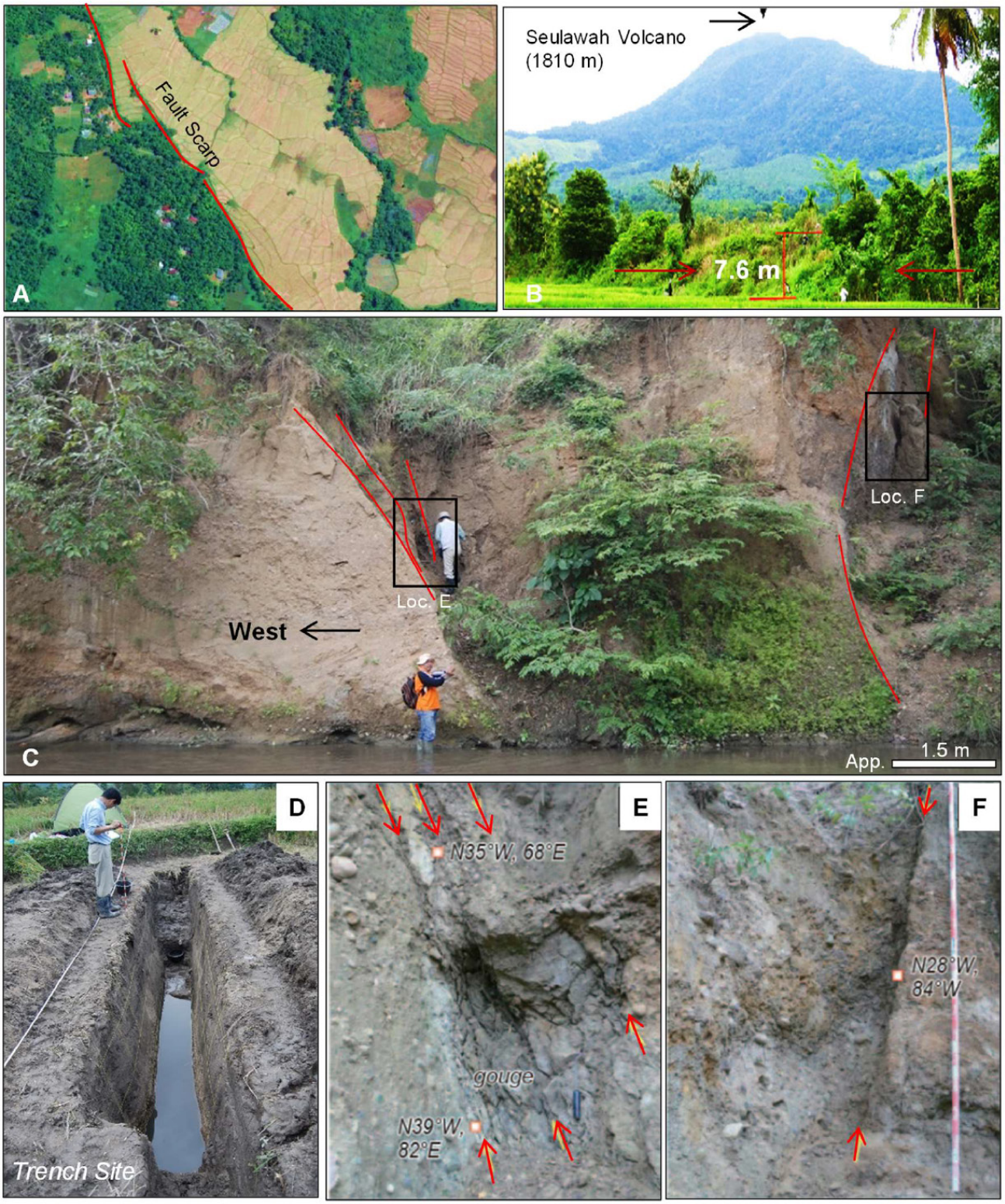

Figure 5: (A) Satellite image from Google observation shows a fault scarp that extends in the same direction as the Seulimeum segment. (B) Photo of the fault scarp with a height of 7.6 m in Lamtamot, Aceh Besar. (C) It is a fault outcrop at the riverbank ~2 km south of Kareung Hill, Lamtamot. (D) Location of the trench site in Lamtamot area, which is the same location in geophysical observation, while (E) and (F) are zoom-in photographs showing, respectively, the gauge and fracture as an outcrop tectonic activity in Kareung Hill.

Seulimeum segment close to the national road of Medan–Banda Aceh. In the middle of the fault segment, the outcrop of the fault scarp with a height of 7.6 m is shown by the geomorphic observation (Figure 5B).

The scrap extends toward the N30°W, which is perpendicular to the direction of the Kareung Hill River. This shows that the scarp originates from the tectonic activity, which has decreased the height in the northwest direction. Image analysis from Google Earth shows that the fault scarp extends in the same direction as the Seulimeum segment fault, passing the rice fields and community settlements (Figure 5A). We also found a Gunong Biram fortress as an ancient site in the 16th century in the fault area. Additionally, several other geomorphic traces were found in the area, including fractures and faults in the same direction as the Seulimeum segment. On the south side of the river, scrap extends in the northwest direction up to ~20 m, called Kareung Hill (Figure 5C). Simultaneously, the outcrops in the black box are represented as a zoom-in of Figures 5(E) and 5(F), which show the gauge and fracture as an outcrop of tectonic activity. The fault is crossing through the southwestern part of the river scarp. Stratigraphically, the scarp layer is formed by sandstones and mudstones that correlate with the Padang Tiji Formation confirmed from geological maps of Aceh Province (Bennett *et al.*, 1981). In more detail, some outcrops on the river scarp are shown in Figures 5(E) and 5(F). The outcrops clearly show the fault of the activity of the Seulimeum tectonic segment. The fault in the Lamtamot village is near the residential zone, school public facilities, mosques, and roads.

Although the regional fault traces can be obtained through topographic differences from satellite imagery, the fault traces cannot be obtained via satellite data in some places where tectonic rates are slow. Therefore, near-surface geophysical measurements should be conducted. Conversely, the mapping of the fault zone can be easily shown by electrical resistivity in some locations with fault gauges and fractures. However, not all sites can be represented by the contrast of resistivity anomaly. The fault zone can be more resistant than the surrounding area if the fault contains minerals such as calcite and quartz. Thus, integrated geophysical methods can image a more accurate fault in the subsurface, since the technique has a different sensitivity depending on the area's geological conditions under study. Based on these geomorphological observations, we performed geophysical studies on the near-fault structure of the Seulimeum segment. Furthermore, we also conducted trenching data with a distance of 4 m and a depth of 1 m with the same location as the geophysical survey.

Geophysical survey

The VLF-EM data provided in- and out-phase parameters oscillated to selected frequencies, 19.8 kHz; however, we only used a single frequency in this study. The out-phase data are an electromagnetic field response that is sensitive to subsurface vertical changes. In contrast, the in-phase data are a magnetic field response sensitive to artificial structural changes that have experienced disturbances due to human activity. These two measurement parameters can be used to examine the characteristics of the shallow faults in the subsurface. Figure 6 shows the in- and out-phase data from measurement results in Lamtamot village, Aceh Besar. Based on the VLF-EM data response, out-phase values are low at 4–28 m along the profile. Furthermore, at 28–42 m along the profile, out-phase values are relatively high given that the anomalous field is perpendicular to the primary magnetic field.

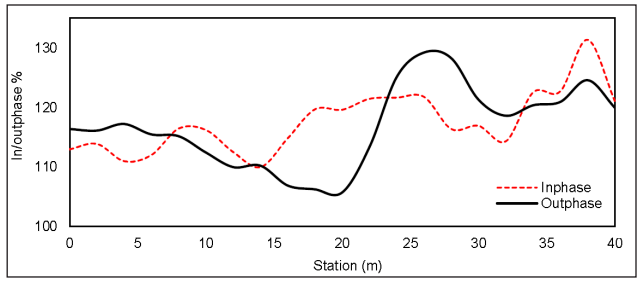

Figure 6: In- and out-phase data provided by the very low frequency-electromagnetic instrument; the fault structure is predicted at distances 16–35 m along the profile.

Additionally, in-phase values at 4–20 m along the profile are relatively low, whereas those at 20–42 m along the profile are relatively high. The intersection point between both data can be used to identify the electrical characteristics of the subsurface conditions. Distances at 12–28 m along the profile could be reflected by conductive material in the subsurface based on the response of in- and out-phase data, whereas those at 28–42 m along the profile are influenced by resistive structures.

According to (Fraser, 1969), vertical subsurface anomalies could be determined through in- and out-phase data intersections. In other words, the VLF-EM data in Lamtamot show that the vertical changes of anomalies at 12–28 m along the profile are expected as a response to a minor fault structure below the subsurface. However, the out- and in-phase data do not provide information about the depth of the structures. Hence, we should still invert the data to obtain the subsurface model of the fault geometry. Karous Hjelt filtering is an inversion method with the principle of discrete filters. The parameter generated from this method is the load density, which is directly proportional to the subsurface electrical conductivity. Karous Hjelt filtering uses a linear filter to solve the integral distribution equation if a horizontal sheet varies with density. Therefore, the longer the trajectory, the greater the assumed depth sheet (Khalil *et al.*, 2009). The depth information obtained in the form of 2-D analytical signals is shown in Eq. 7:

$$(\Delta z/2\pi)I_a(\Delta x/2) = -0.205H_{-2} + 0.323H_{-1} - 1.446H0 + 1446H_1 - 0.323H_2 + 0.205\, H_3\, I_a\,(x/2), \quad (7)$$

where Δz is the assumption of the thickness in a layer for the cross-sectional area of the charge density; Δ*x* is the distance between measurement data points and used as the depth in a layer, while H_{-2} to H_{-3} is the vertical normalizations of the magnetic field ($H_{Z/}H_{Y}$) at six measurement data points. The filter provides the depth information of electrical current due to subsurface responses such as fracture zones, fault, and other geological objects in the subsurface. The qualitative analysis of VLF-EM data was conducted using KHFfilt software developed by Oulu University (Pirttijärvi, 2004). It should be noted that the Karous Hjelt filtering application has been widely used to estimate subsurface structures, e.g., in the Indian region, to identify groundwater (Kumar *et al.*, 2016) and archaeological structures in the subsurface. In this study, the electrical current density was calculated using the KHFfilt software and the out- and in-phase data transformed to the electrical charge density, making the data directly proportional to subsurface electrical conductivity properties. The electric charge data will be inversely proportional to the resistivity parameter of the ERT method, which has been measured at the same location as that of the VLF-EM method. Furthermore, Figure 7 shows the depth estimation anomaly obtained via Karous Hjelt filtering and the comparison of the model with the 2D electrical resistivity and magnetic data.

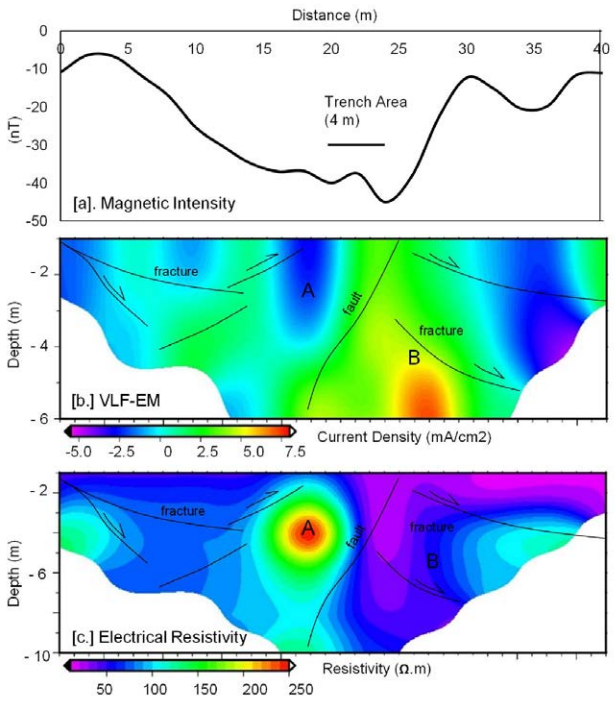

Figure 7: Comparison of the very low frequency-electromagnetic (VLF-EM) data with another geophysical method crossing the Seulimeum segment. (a) The anomaly of total intensity magnetic has been reduced to the pole. The black line has also shown the trenching area in geophysical surveys. (b) Two-dimensional (2-D) inverted current density model derived from the VLF-EM method. (c) The 2-D resistivity model inverted from the electrical resistivity data measured in the same profile.

The 2-D inverted VLF-EM data model (Figure 7b) shows a relatively high current density at 8–20 m along the profiles of 6 m depth. The inverted model of VLF-EM agrees with the ERT model represented by low resistivity anomalies. The uppermost layer is interpreted as fluvial deposits. Regarding (Khalil *et al.*, 2009), high current density data are associated with the subsurface conductive layer. Conversely, at 20–35 m along the profile, the current density data are relatively low at 2–4 m depth (i.e., indicated by symbol A). In contrast, at 4–6 m depth, the current density data are high (shown by the B symbol). This high-density current zone also agrees with the most resistive model derived from the ERT method, where there is a high-value resistivity of 200–250 Ωm at 15–20 m and a low value of 50–100 Ωm at 20–35 m. This anomaly is a response to the shallow fault, which is also mapped via the VLF-EM method. It can be interpreted as volcanic lava rocks found at 20–24 m along the profiles based on resistivity value.

The conductive layer at the same depth of 24–32 m along the profile is interpreted as sand and gravel layers. The vertical changes of resistive and conductive zones at ~24 m along the profile can be interpreted as a shallow fault structure within the subsurface. The shallow fault can also be indicated by the response of the magnetic intensity data (Figure 7a), which change significantly, from a low value (i.e., −20 to −40 nT) at 5–25 m to an increased value (from −40 to −10 nT) at 25–30 m from the profile. Assuming the direction of the magnetization is the same as the direction of the regional magnetic field, the data would have been reduced to the poles with an inclination of −5.21°, a declination of −0.77°, and a total field of 41.737 nT obtained from the World Magnetic Model.

According to (Grauch *et al.*, 2006; Nasuti *et al.*, 2012), vertical anomalies such as dykes and faults can be characterized by contrasting changes in the total magnetic field. Additionally, the data presented in Figure 7(a) are the magnetic responses, which are reduced to the pole. We applied this technique to obtain a monopole anomaly that can be directly interpreted in the geological object. Nevertheless, the magnetic data can only show the fault's location without the depth information from the anomaly. Hence, further data processing is warranted. The integration of the VLF-EM method with the ERT and magnetic methods also shows some fractures as seismic activity at the Lamtamot area. For example, at 5–15 m, a current density contrast is elucidated through resistivity data; the 2-D model shows that the depth fracture is ~2–6 m, but the magnetic field intensity data are unable to show the different responses of the anomaly. Additionally, at 30–35 m, the fracture is mapped by the contrast of current density shown from the resistivity and magnetic field data.

Comparison to trenching data

Based on the trenching data excavated at a depth of 1 m (Figure 8), seven layers were obtained with different

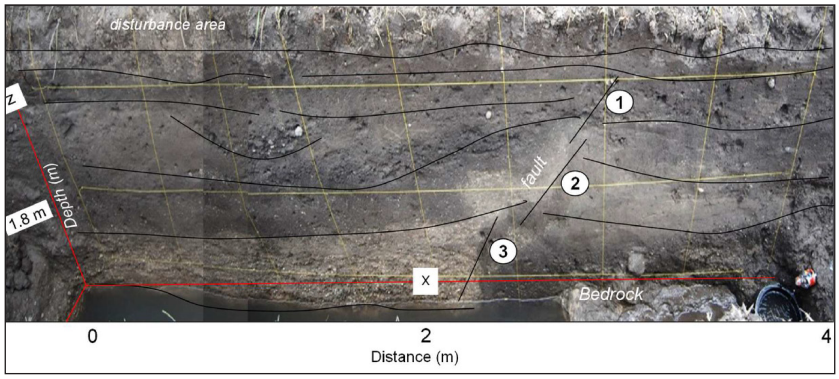

Figure 8: Trench site data that show the subsurface layer in 1.8 m depth. The number in the figure is represented as a possible fracture or shallow fault in the subsurface.

characteristics. The first layer is dominated by a disturbance layer with a thickness of ±20 cm, indicating disruption caused by agricultural activities. Layer two is dominated by sand from fine to medium size with brownish color, where the sand layer contains pebble with a round texture of 4 cm size. At the top of the second layer, there are root traces that indicate that it was formerly paleosoil. The third layer is in the form of fine sand, brown to brass in color. The boundary between layers two and three is gradual and irregular, and there are several deposits of former canals containing round to round pebbles. It is a pebble with a brown to gray color in layer four, a deposit matrix of spherical shape with a diameter of 4 cm. This layer only exists in the eastern part of the trenching. The fifth layer consists of fine sand to brown silt, and this layer contains several pebbles with a size of less than 5 cm. This layer is thin in the eastern part and disturbed in the fault zone and the western part. The sixth layer is fine sand brown to yellow brass containing a pebble of less than 1 cm. In this layer, there is a distribution of spiral-shaped shells.

Generally, the interpretation of the geophysical model cannot distinguish the resistivity of the layers because all these layers have a resistivity value in the same range. However, the measurement location is precisely in the fault zone, which causes the water to fill the fracture so that the two geophysical methods can map well structures that are fault and crack. It is relatively conductive compared to other materials since the zone is filled with water. The advantage of geophysical measurements is that they are more sensitive to structures than differences between dry and water-saturated areas.

CONCLUSION

The VLF-EM method has been conducted to map the Seulimeum segment's shallow fault in Lamtamot, Aceh Province. Compared with other geophysical methods such as ERT and magnetic methods, the conventional technique has been widely applied to study shallow faults in the subsurface. We also present geomorphological observations for mapping the traces of fault seismicity. Our results show that the Seulimeum segment is an active fault that directly crosses the development activities and human settlements. Based on the analysis of the current density from the VLF-EM method, the data show the shallow fault at a distance of 20–32 m from profile measurement and a depth of 2–8 m in the subsurface. Furthermore, the anomaly correlates with the resistivity data from the ERT method and the magnetic field intensity from the magnetometer measurement. The 2-D model from VLF-EM and ERT data also shows some fractures that reflect the tectonic activity, such as 5–15 m and 30–35 m from the measurement profile. Based on the result of the comparison, it can be concluded that the VLF-EM can be used to investigate the shallow fault structures. Moreover, the data comparison from VLF-EM, magnetic, and ERT methods has shown a similar pattern anomaly from the geological structure in the subsurface. Further, compared with the ERT method, practical data acquisition via the VLF-EM method is considerably faster and more useful for a large area.

ACKNOWLEDGEMENTS

Thanks to the geophysics and physics department students who helped during the fieldwork in Lamtamot, Aceh Besar. This research was funded by the Directorate of Higher Education, Ministry of Education and Culture, Indonesia under a Research Basis grant with contract number No: 6/UN11.2.1/PT.01.03/DRPM/2020. The authors would like to thank Prof. Hiroyuki Tsutsumi and Yoshio Soeda for their support. We also thank the reviewers who have provided many suggestions for a better and quality paper, that can be accepted by the Bulletin of the Geological Society of Malaysia.

AUTHOR CONTRIBUTIONS

MY and GI participated in the study design. NI and MY did the statistical analysis and drafted the manuscript. GI made the filtering of VLF-EM and magnetic data, while NI and MY contributed to the interpretation of the geophysical and geological models. All authors read and approved the final manuscript.

CONFLICT OF INTEREST

The authors declare that we have no conflict of interest in this paper.

REFERENCES

Abbas, A.M., Khalil, M.A., Massoud, U., Santos, F.M., Mesbah, H.A., Lethy, A., Soliman, M. & Ragab, E.S.A., 2012. The implementation of multi-task geophysical survey to locate Cleopatra Tomb at Tap-Osiris Magna, Borg El-Arab, Alexandria, Egypt "Phase II". NRIAG J. Astron. Geophys., 1(1), 1-11. https://doi.org/10.1016/j.nrjag.2012.11.001.

Baranwal, V.C. & Sharma, S.P., 2006. Integrated geophysical studies in the East-Indian geothermal province. Pure Appl. Geophys., 163, 209-227. https://doi.org/10.1007/s00024-005-0001-2.

Bennett, J.D., Bridge, N.R., Djunuddin, A., Ghazali, S.A., Jeffery, D.H., Keats, W., Rock, N.M.S., Thompson, S.J. & Whandoyo, R., 1981. The geology of the Banda Aceh Quadrangle, Sumatra. Geological Research and Development Centre, Bandung. Explan. note 19.

Bichler, A., Bobrowsky, P., Best, M., Douma, M., Hunter, J., Calvert, T. & Burns, R., 2004. Three-dimensional mapping of a landslide using a multi-geophysical approach: the Quesnel Forks landslide. Landslides, 1, 29–40. https://doi.org/10.1007/s10346-003-0008-7.

Bosch, F.P. & Müller, I., 2001. Continuous gradient VLF measurements: A new possibility for high resolution mapping of karst structures. First Break, 19(6), 343-350. https://doi.org/10.1046/j.1365-2397.2001.00173.x.

Chabaane, A., Redhaounia, B. & Gabtni, H., 2017. Combined application of vertical electrical sounding and 2D electrical resistivity imaging for geothermal groundwater characterization: Hammam Sayala hot spring case study (NW Tunisia). J. African Earth Sci., 134, 292-298. https://doi.org/10.1016/j.jafrearsci.2017.07.003.

Chatterjee, S., Bhattacharyya, R., Michael, L., Krishna, K.S. & Majumdar, T.J., 2007. Validation of ERS-1 and high-resolution satellite gravity with in-situ shipborne gravity over the Indian offshore regions: Accuracies and implications to subsurface modeling. Mar. Geod., 30, 197–216. https://doi.org/10.1080/01490410701438323.

Ebrahimi, A., Sundararajan, N. & Ramesh Babu, V., 2019. A comparative study for the source depth estimation of very low frequency electromagnetic (VLF-EM) signals. J. Appl. Geophys., 162, 174-183. https://doi.org/10.1016/j.jappgeo.2019.01.007.

Fernández-Blanco, D., Philippon, M. & Von Hagke, C., 2016. Structure and kinematics of the Sumatran fault system in North Sumatra (Indonesia). Tectonophysics, 693, 453–464.

Fraser, D.C., 1969. Contouring of VLF-EM Data. Geophysics, 34(6), 958-967. https://doi.org/10.1190/1.1440065.

GEM Systems, 2015. Instruction manual release GSM-19 v7.0. GEM Systems, Inc., Canada. 148 p.

Grauch, V.J.S., Hudson, M.R., Minor, S.A. & Caine, J.S., 2006. Sources of along-strike variation in magnetic anomalies related to intrasedimentary faults: A case study from the Rio Grande Rift, USA. Explor. Geophys., 37, 372-378. https://doi.org/10.1071/EG06372.

Gürer, A., Bayrak, M. & Gürer, Ö.F., 2009. A VLF survey using current gathering phenomena for tracing buried faults of Fethiye-Burdur Fault Zone, Turkey. J. Appl. Geophys., 68(3), 437-447. https://doi.org/10.1016/j.jappgeo.2009.03.011.

Ismail, N., Yanis, M., Idris, S., Abdullah, F. & Hanafiah, B., 2017. Near-surface fault structures of the Seulimuem segment based on electrical resistivity model. Journal of Physics: Conference Series, 846, 012016. https://doi.org/10.1088/1742-6596/846/1/012016.

Ito, T., Gunawan, E., Kimata, F., Tabei, T., Simons, M., Meilano, I., Agustan, Ohta, Y., Nurdin, I. & Sugiyanto, D., 2012. Isolating along-strike variations in the depth extent of shallow creep and fault locking on the northern Great Sumatran Fault. J. Geophys. Res. Solid Earth, 117(6), B06409. https://doi.org/10.1029/2011JB008940.

Kamesh Raju, K.A., Murty, G.P.S., Amarnath, D. & Kumar, M.L.M., 2007. The west Andaman fault and its influence on the aftershock pattern of the recent megathrust earthquakes in the Andaman-Sumatra region. Geophys. Res. Lett., 34, L03305. https://doi.org/10.1029/2006GL028730.

Karcıoğlu, G., 2019. Near-surface resistivity structure near avcilar landslide in İstanbul, Turkey by 2D inversion of VLF data. J. Appl. Geophys., 163, 73-83. https://doi.org/10.1016/j.jappgeo.2019.02.012.

Khalil, M.A., Santos, F.A.M., Moustafa, S.M. & Saad, U.M., 2009. Mapping water seepage from lake nasser, Egypt, using the VLF-EM method: A case study. J. Geophys. Eng., 163, 73-83. https://doi.org/10.1088/1742-2132/6/2/001.

Kumar, D., Ramadass, G. & Jagadish., S.V., 2016. A quantitative analysis of VLF data for groundwater exploration in a hardrock terrain in Osmania University Campus, Hyderabad, Telangana State, India. Int. J. Adv. Res., 4(9), 802-821. https://doi.org/10.21474/ijar01/1549.

Loke, M.H. & Lane, J.W., 2004. Inversion of data from electrical resistivity imaging surveys in water-covered areas. Explor. Geophys., 35(4), 266-271. https://doi.org/10.1071/EG04266.

Ma, G. & Li, L., 2012. Edge detection in potential fields with the normalized total horizontal derivative. Comput. Geosci., 41, 83-87. https://doi.org/10.1016/j.cageo.2011.08.016.

Martí, A., Queralt, P., Marcuello, A., Ledo, J., Rodríguez-Escudero, E., Martínez-Díaz, J.J., Campanyà, J. & Meqbel, N., 2020. Magnetotelluric characterization of the Alhama de Murcia Fault (Eastern Betics, Spain) and study of magnetotelluric interstation impedance inversion. Earth, Planets Sp., 72(1), 19 p. https://doi.org/10.1186/s40623-020-1143-2.

Marwan, Asrillah, Yanis, M. & Furumoto, Y., 2019a. Lithological identification of devastated area by Pidie Jaya earthquake through Poisson's Ratio analysis. Int. J. GEOMATE, 17(63), 210–216. https://doi.org/10.21660/2019.63.77489.

Marwan, Yanis, M., Idroes, R. & Ismail, N., 2019b. 2D inversion and static shift of MT and TEM data for imaging the geothermal resources of Seulawah Agam Volcano, Indonesia. Int. J. GEOMATE, 17(62), 173–180. https://doi.org/10.21660/2019.62.11724.

Muzli, M., Muksin, U., Nugraha, A.D., Bradley, K.E., Widiyantoro, S., Erbas, K., Jousset, P., Rohadi, S., Nurdin, I. & Wei, S., 2018. The 2016 Mw 6.5 Pidie Jaya, Aceh, North Sumatra, earthquake: Reactivation of an unidentified sinistral fault in a region of distributed deformation. Seismol. Res. Lett., 89(5), 1761-1772. https://doi.org/10.1785/0220180068.

Nasuti, A., Pascal, C. & Ebbing, J., 2012. Onshore-offshore potential field analysis of the Møre-Trøndelag Fault Complex and adjacent structures of Mid Norway. Tectonophysics, 518-521, 17-28. https://doi.org/10.1016/j.tecto.2011.11.003.

Natawidjaja, D.H. & Triyoso, W., 2007. The Sumatran fault zone—From source to hazard. J. Earthq. Tsunami, 1, 21–47.

Niculescu, B.M. & Andrei, G., 2019. Using vertical electrical soundings to characterize seawater intrusions in the southern area of Romanian Black Sea coastline. Acta Geophysica, 67, 1845–1863. https://doi.org/10.1007/s11600-019-00341-y.

Olesen, O., Henkel, H., Lile, O.B., Maruing, E., Ronning, J.S. & Torsvik, T.H., 1992. Netotectonics in the Precambrian of Finnmark, northern Norway. Nor. Geol. Tidsskr, 72, 301-306.

Pirttijärvi, M., 2004. Karous-Hjelt and Fraser filtering of VLF measurements - Manual of the KHFFILT program. University of Oulu, Finland.

Pozdnyakova, L., Pozdnyakov, A. & Zhang, R., 2001. Application of geophysical methods to evaluate hydrology and soil properties in urban areas. Urban Water, 3, 205-216. https://doi.org/10.1016/S1462-0758(01)00042-5.

Ramesh Babu, V., Ram, S. & Sundararajan, N., 2007. Modeling and inversion of magnetic and VLF-EM data with an application to basement fractures: A case study from Raigarh, India. Geophysics, 72(5), B133-B140. https://doi.org/10.1190/1.2759921.

Rizal, M., Ismail, N., Yanis, M., Muzakir & Surbakti, M.S., 2019. The 2D resistivity modelling on north Sumatran fault structure by using magnetotelluric data. IOP Conf. Ser. Earth Environ. Sci., 364(1), 12036. https://doi.org/10.1088/1755-1315/364/1/012036.

Saibi, H., Aboud, E. & Ehara, S., 2012. Analysis and interpretation of gravity data from the Aluto-Langano geothermal field of Ethiopia. Acta Geophys., 60, 318–336. https://doi.org/10.2478/s11600-011-0061-x.

Sieh, K. & Natawidjaja, D., 2000. Neotectonics of the Sumatran fault, Indonesia. J. Geophys. Res. Solid Earth, 105, 28295–28326. https://doi.org/10.1029/2000JB900120.

Sundararajan, N., Ramesh Babu, V., Shiva Prasad, N. & Srinivas, Y., 2006. VLFPROS-A Matlab code for processing of VLF-EM data. Comput. and Geosci., 32(10), 1806-1813. https://doi.org/10.1016/j.cageo.2006.02.021.

Sungkono, Husein, A., Prasetyo, H., Bahri, A.S., Monteiro Santos, F.A. & Santosa, B.J., 2014. The VLF-EM imaging of potential collapse on the LUSI embankment. Journal of Applied Geophysics, 109, 218–232. https://doi.org/10.1016/j.jappgeo.2014.08.004.

Surya, R.A., Abdullah, F., Darisma, D., Yanis, M. & Ismail, N., 2019. Sedimentation process in Kuala Gigieng coast, Aceh Besar based on magnetic and gravity surveys. IOP Conf. Ser. Earth Environ. Sci., 348, 12040. https://doi.org/10.1088/1755-1315/348/1/012040.

Telford, W.M., Geldart, L.P. & Sheriff, R.E., 1990. Applied geophysics. Cambridge University Press, Cambridge, New York, Australia. 751 p. https://doi.org/10.1017/CBO9781139167932.

USGS, 2020. Earthquake Catalog [WWW Document]. URL https://earthquake.usgs.gov/earthquakes/search/ (accessed 1.1.20).

Yanis, M., A Bakar, M. & Ismail, N., 2017. The use of VLF-EM and electromagnetic induction methods for mapping the ancient fort of Kuta Lubok as tsunami heritage i. Conference Proceedings, 23rd European Meeting of Environmental and Engineering Geophysics, 2017, 1-5. https://doi.org/10.3997/2214-4609.201701996.

Yanis, M., Abdullah, F., Zaini, N. & Ismail, N., 2021. The northernmost part of the Great Sumatran Fault map and images derived from gravity anomaly. Acta Geophys., 69, 795–807. https://doi.org/10.1007/s11600-021-00567-9.

Yanis, M., Faisal, A., Yenny, A., Muzakir, Z., Abubakar, M. & Nazli, I., 2020. Continuity of Great Sumatran Fault in the marine area revealed by 3D inversion of gravity data. J. Teknol., 83, 145–155. https://doi.org/10.11113/jurnalteknologi.v83.14824.

Yanis, M. & Marwan, 2019. The potential use of satellite gravity data for oil prospecting in Tanimbar Basin, Eastern Indonesia. IOP Conf. Ser. Earth Environ. Sci., 364, 12032. https://doi.org/10.1088/1755-1315/364/1/012032.

Yanis, M., Zainal, M., Marwan, M. & Ismail, N., 2019. Delineation of buried paleochannel using EM induction in Eastern Banda Aceh, Indonesia. https://doi.org/10.3997/2214-4609.201900705.

Yanis, M., Marwan & Ismail, N., 2019. Efficient use of satellite gravity anomalies for mapping the Great Sumatran Fault in Aceh Province. Indonesian J. Appl. Phys., 9, 61. https://doi.org/10.13057/ijap.v9i2.34479.

Zainal, M., Yanis, M., Darisma, D., Marwan & Ismail, N., 2019. The determination of depth anomaly in archaeo-magnetic using an Euler deconvolution: Case study in Kuta Lubok fortress. IOP Conf. Ser. Earth Environ. Sci., 364, 12034. https://doi.org/10.1088/1755-1315/364/1/012034.

Zhang, L., Unsworth, M., Jin, S., Wei, W., Ye, G., Jones, A.G., Jing, J., Dong, H., Xie, C., Le Pape, F. & Vozar, J., 2015. Structure of the Central Altyn Tagh Fault revealed by magnetotelluric data: New insights into the structure of the northern margin of the India-Asia collision. Earth Planet. Sci. Lett., 415, 67-79. https://doi.org/10.1016/j.epsl.2015.01.025.

Manuscript received 4 March 2021;
Received in revised form 28 August 2021;
Accepted 6 September 2021
Available online 19 May 2022